# Rationalizing the Grain Size Dependence of Strength and Strain-Rate Sensitivity of Nanocrystalline fcc Metals

Y.Z. LI and M.X. HUANG

Low strain-rate sensitivity (SRS) of nanocrystalline metals measured by experiments often leads to the claim that grain boundary (GB)-mediated plasticity is insignificant, contrary to molecular dynamics simulation results. Here, we develop an crystal plasticity model to rationalize the important role of GB-mediated plasticity on the rate-controlling deformation of nano-grained (NG) and ultrafine-grained (UFG) face-centered-cubic (fcc) metals. Important phenomena such as the GB strengthening, the stress saturation, and the evolution of SRS are well captured. We show that the main reason for the low SRS measured experimentally in NG metals (several tens of nm) is the dominance of the localized dislocation activities over the GB process on the overall plasticity. Such localization of dislocation process may provide a reason for the formation of shear bands/zones in NG and UFG fcc metals.

https://doi.org/10.1007/s11661-019-05112-4


IT is well known that grain size can significantly influence the mechanical properties of polycrystalline metals and alloys.[1] The conventional plasticity mechanism in coarse-grained (CG) face-centered-cubic (fcc) metals, mediated by the nucleation and gliding of dislocations in the grain interior,[2] is expected to become increasingly difficult with reduction of grain size down to the nanometer regime characterized by the abundant grain boundary (GB) atoms.[3] Studies[4–6] have shown that grain refinement in the ultrafine-grained (UFG) or nano-grained (NG) regimes leads to an obvious strengthening effect, which appears to follow the well-established Hall-Petch (HP) relationship[7,8] originally proposed to describe CG metals, *i.e.*,

$$\sigma_y = \sigma_\infty + kd^{-1/2} \quad [1]$$

where $\sigma_y$ is the yield stress, $\sigma_\infty$ is the stress at which yielding occurs at very large grain sizes, $k$ is the slope, and $d$ is the average grain size. Such an empirical equation has been explained mostly by dislocation-based models including (i) stress concentrations induced by dislocation pileups[7,9] and (ii) Taylor's relation $\sigma_y \propto \sqrt{\rho}$ together with the assumption of $\rho \propto 1/d$ where $\rho$ is dislocation density.[10,11] However, these explanations suffer from the fact that metals either without pileups or exhibiting the starvation of dislocations[12] nevertheless obey this HP form. This contradiction naturally leads to a new view that the hardening of nanostructured metals may be induced by an additional deformation mechanism associated with numerous GBs.

Molecular dynamics simulations[2,13,14] indicate that the GB-mediated plasticity (*e.g.*, GB sliding[15,16] and/or diffusion[3]) serves as the cooperating/competing mechanism to the conventional dislocation slip when grain sizes are reduced below a critical value. Although direct experimental observations for such a transition are lacking, indirect experimental evidences based on the rate behavior of UFG/NG fcc metals hint at this GB mechanism.[17] The strain rate sensitivity (SRS) index $m$, which serves as a signature of deformation mechanism,[18] is typically $0.005 - 0.01$ for CG fcc metals such as Cu,[19] Ni,[20] and Al.[21] Although $m$ is generally insensitive to grain size in the micrometer regime, it has been discovered that further refining microstructures to nanometer regime will lead to an elevated $m$. In particular, the $m$ value at $d \sim 30$ nm is measured to be 0.02 for NG-Ni[20] and 0.035 for NG-Cu.[22,23] Yet, these values are still much lower than that corresponding to the GB-mediated plasticity ($m = 0.5 - 1$), and this often leads to the claim from some investigators[20,23] that GB activities are not important even in NG metals. Given such a controversy between simulation results and experimental suggestions, it is natural to ask to what degree does the experimentally measured $m$ really reflect the GB-mediated plasticity. Surprisingly, until now no

Y.Z. LI and M.X. HUANG are with the Department of Mechanical Engineering, The University of Hong Kong, Pokfulam Road, Hong Kong, China and also with the Shenzhen Institute of Research and Innovation, The University of Hong Kong, Shenzhen, China. Contact e-mail: mxhuang@hku.hk
Manuscript submitted November 10, 2018.
Article published online January 23, 2019

well-accepted explanation seems to exist. Here, we bring a new insight into the deformation mechanism of nanocrystalline fcc metals by rationalizing the role of GBs as an cooperative rate-controlling deformation process subsidiary to the dislocation slip. The present new crystal plasticity model allows us to quantitatively predict the gradual increase of $\sigma_y$ and $m$ with decreasing $d$, and also to capture important phenomenon such as the saturation of yield stress and the rapid transition of $m$ at extremely small grain sizes ($d < 15$ nm). The model may shed new light on understanding the occurrence of shear bands/zones in UFG/UG metals.

The present discussion relies on the facts that (i) the grain size as well as the spacing between neighboring dislocations follow a statistical distribution rather than one single value, and (ii) the GB-mediated plasticity typically with $m = 0.5$–$1$ and higher mechanical threshold stress,[24] regardless of its specific form such as sliding or diffusion, will eventually contribute to the overall plasticity at small grain sizes due to dislocation starvation.

The conventional dislocation plasticity of CG fcc metals can be characterized by the power-law behavior, which connects the shear strain rate $\dot{\gamma}$ to the applied shear stress $\tau$ according to $\tau/\hat{\tau} = (\dot{\gamma}/\hat{\dot{\gamma}})^m$,[25] where $\hat{\dot{\gamma}}$ is the reference strain rate, $\hat{\tau}$ is the mechanical threshold stress serving as an internal variable, and $m$ is the SRS index for the deformation mechanism controlled by slip. This power law is applicable when enough nucleation and motion of dislocations occur in the grain interior. Further reducing grain sizes to a certain level will inevitably activate the GB-mediated plasticity,[3,26] as intra-grain dislocation sources are inadequate to accommodate the macroscopic deformation response. We thereby formalize this rationale by consolidating the two deformation processes into one general form, which accounts for the coexistence of both the conventional dislocation mechanism inside grain interiors and the GB-mediated mechanism:

$$\dot{\gamma} = \underbrace{\hat{\dot{\gamma}}_{\text{disl}}\left(\frac{\tau}{\hat{\tau}_{\text{disl}}}\right)^{1/m_{\text{disl}}}\phi}_{\dot{\gamma}_{\text{disl}}} + \underbrace{\hat{\dot{\gamma}}_{\text{GB}}\left(\frac{\tau}{\hat{\tau}_{\text{GB}}}\right)^{1/m_{\text{GB}}}\left(1-\phi\right)}_{\dot{\gamma}_{\text{GB}}} \quad [2]$$

where the subscripts "disl" and "GB" denote the conventional dislocation process and the GB-mediated plasticity, respectively, and $\phi$ is the nondimensional parameter reflecting the volume fraction of grains deformed by dislocation slip. The form of Eq. [2] relies on the fact that the coupling between dislocation-based mechanism and GB-mediated plasticity enforces the compatibility and equilibrium on the overall deformation. For CG metals at low applied stresses $\phi \sim 1$ and $\tau/\hat{\tau}_{\text{GB}} \ll 1$, Eq. [2] will be reduced to the original power law.

Since the rate-sensitivity index $m$ is experimentally measured according to $m = \partial \ln \tau / \partial \ln \dot{\gamma}$, it is now related to both $m_{\text{disl}}$ and $m_{\text{GB}}$ and therefore should be regarded as an apparent value rather than the signature of a specific deformation process. Based on Eq. [2], the general expression of the overall sensitivity index $m$, which is measured experimentally, becomes

$$m = \frac{1+\lambda}{m_{\text{disl}}/m_{\text{GB}} + \lambda} m_{\text{disl}} \quad [3]$$

where the nondimensional index $\lambda$ responsible for the final value of $m$ is expressed as

$$\lambda = \frac{\phi}{1-\phi}\left(\frac{\tau}{\hat{\tau}_{\text{disl}}}\right)^{1/m_{\text{disl}}}\left(\frac{\hat{\tau}_{\text{GB}}}{\tau}\right)^{1/m_{\text{GB}}} \quad [4]$$

Two cases of $\lambda(\phi)$ are evident: $\phi = 1$ for CG metals leading to $\lambda = \infty$ and $m = m_{\text{disl}}$, and $\phi = 0$ for extremely small grains (*e.g.*, $d$ a few nanometers) causing $\lambda = 0$ and $m = m_{\text{GB}}$.

The volume fraction $\phi$ of slip-controlled grains is generally an increasing function of the average grain size $d$. To derive the explicit expression of $\phi(d)$, we consider the real homogeneous crystalline structures in which the accurate grain size $\tilde{d}$ and the dislocation spacing $\tilde{l}$ have frequency distributions. In this case, the probability density functions (PDFs) of grain size $P(\tilde{d})$ and dislocation spacing $P(\tilde{l})$ follow a log-normal distribution, as experimentally verified[20] and extensively used in numerical approaches[15,27–29] that writes

$$P(\tilde{d}) = \frac{1}{\sqrt{2\pi}s\tilde{d}}\exp\left(-\frac{1}{2}\left(\frac{\ln(\tilde{d}/d_0)}{s}\right)^2\right) \quad [5]$$

and

$$P(\tilde{l}) = \frac{1}{\sqrt{2\pi}s\tilde{l}}\exp\left(-\frac{1}{2}\left(\frac{\ln(\tilde{l}/l_0)}{s}\right)^2\right) \quad [6]$$

where $s$ is the standard deviation calibrated as 0.1 by referring to the available grain size distribution (Figure 1(a)), and $d_0$ and $l_0$ are the median values relating to the arithmetic mean values $d$ and $l$ respectively by $d = d_0 \exp(s^2/2)$ and $l = l_0 \exp(s^2/2)$. For simplicity, we assume here that $P(\tilde{l})$ follows the same shape ($s$ value) as $P(\tilde{d})$. Note that Eqs. [5] and [6] cannot be applied to heterogeneous materials with bimodal grain size distributions or with grain size gradient regions. For a single grain (denoted as $i$) with the size $\tilde{d}_i$, the conventional dislocation plasticity takes place if it contains dislocations inside, which requires the local dislocation spacing $\tilde{l}_i \le \tilde{d}_i$. The probability $p$ for such a case (having dislocations inside a grain) can be expressed by $p_i(\tilde{d}_i) = \int_0^{\tilde{d}_i} P(\tilde{l})d\tilde{l}$. The volume fraction $\phi$, according to its definition, can be derived by averaging this probability $p_i$ over all the $N$ numbers of grains as

$$\phi = \frac{1}{N}\sum_{i=1}^{N} p_i \overset{N\to\infty}{=} \int_0^{\infty}\int_0^{\tilde{d}} P(\tilde{d})P(\tilde{l})d\tilde{l}d\tilde{d} \quad [7]$$

Equation [7] together with Eqs. [5] and [6] gives the analytical expression of $\phi$ depending on the average grain size $d$ and the average dislocation spacing $l$. For

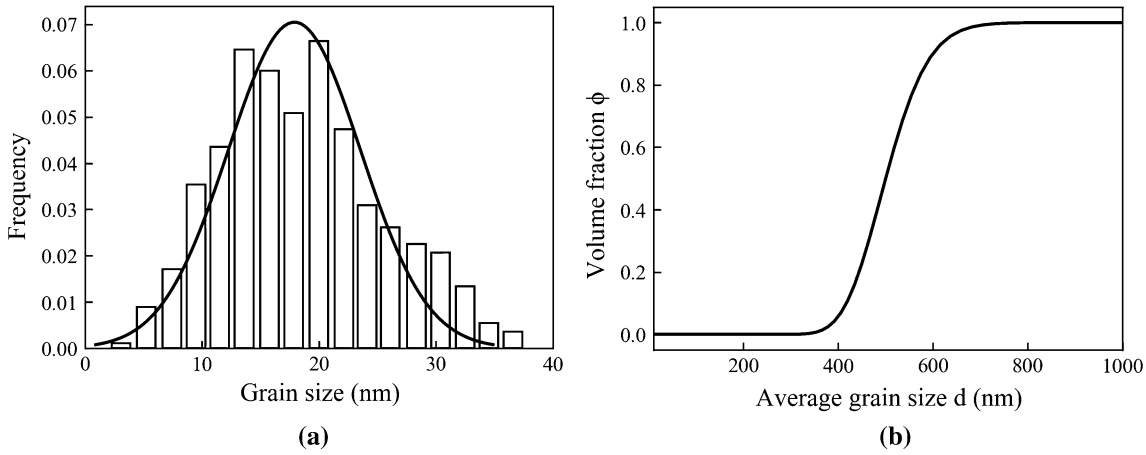


Fig. 1—(*a*) Grain size distribution (bar) according to the data from Ref. [30] fitted with a lognormal distribution function (solid line) with $d_0$ = 17.9 nm and $s = 0.1$. (*b*) Variation of $\phi$ with the average grain size $d$ computed from Eq. [7].

undeformed metals with dislocation density $\rho \sim 10^{12} - 10^{13}$ m$^{-2}$, the average spacing $l \sim 300$–1000 nm according to $l \sim \rho^{-1/2}$.

Figure 1(b) shows the variation of $\phi$ with the average grain size $d$, computed from Eq. [7] with $l = 500$ nm (assuming $\rho = 4 \times 10^{12}$ m$^{-2}$). At relatively large grain sizes, *i.e.*, $d$ close to 1 $\mu$m, $\phi \sim 1$ and Eq. [2] in this case reduces to the conventional power law, suggesting that intra-grain dislocation motions take place everywhere and govern the macroscopic plasticity. With further grain size reduction, $\phi$ starts to drop at $d \sim 600$ nm until $\phi$ reaches a small value of $\sim 0.06$ at $d \sim 400$ nm, indicating that the intra-grain dislocation activities are now confined in a limited number of grains still containing dislocations. It should be noted that the parameter $\phi$ merely reflects the volume percentage of grains deformed by conventional dislocation process. In other words, the small value of $\phi$ does not necessarily correspond to the dominance of GB-mediated plasticity over the dislocation plasticity.[31] Details of this aspect will be discussed further.

After knowing the relationship between $\phi$ and $d$ (Figure 1(b)), Eq. [2] is further evaluated by calculating the yield stress $\sigma_y$ for any fcc metal with different grain sizes. For illustrative purposes, we consider the most widely used model material Cu.[32] deformed at a fixed strain rate $\dot{\gamma} = 5 \times 10^{-4}$ s$^{-1}$[29] which is experimentally accessible. The typical values $m_{\text{disl}} = 0.005$ and $m_{\text{GB}} = 1$[33] are chosen for Cu. The mechanical threshold stress $\hat{\tau}_1$ and $\hat{\tau}_2$ are assigned as 40 MPa[34] and 600 MPa, respectively. To compute $\sigma_y$, we use the relationship $\sigma_y = M\tau_y$ where $M \sim 3$ is the Taylor factor for polycrystals without texture.[35]

Figure 2 shows the calculated yield stress $\sigma_y$ *vs* $d^{-1/2}$ based on Eq. [2] for Cu. The values of $\dot{\gamma}_{0,1}$ and $\dot{\gamma}_{0,2}$ are chosen in order to fit the experimental data, which are also presented in Figure 2 for comparison. The best fit is $\dot{\gamma}_{0,1} = 10^{-5}$ s$^{-1}$ and $\dot{\gamma}_{0,2} = 10^{-3}$ s$^{-1}$. In Figure 2, the calculated $\sigma_y$ *vs* $d^{-1/2}$ relation (solid line) exhibits a nonlinear behavior, which deviates from the straight HP line (dashed line in Figure 2) extrapolated from

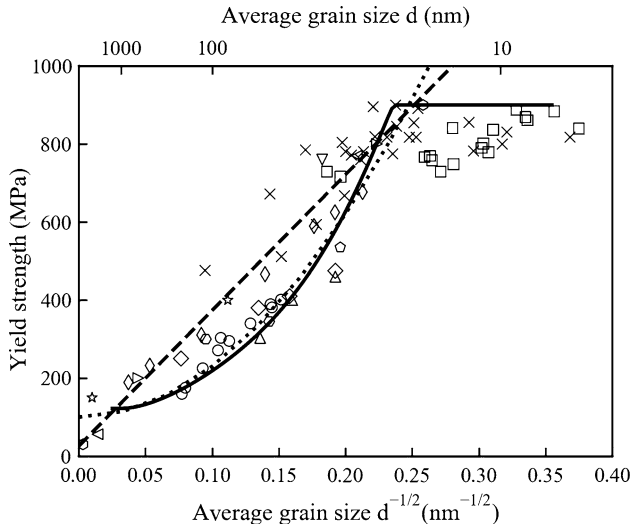


Fig. 2—The yield stress $\sigma_y$ *vs* $d^{-1/2}$ (solid line) computed from Eq. [2], in comparison with experimental data (symbols) from literature for UFG/NG Cu. Dashed line: the HP relationship extrapolated from CG-Cu[36]; Dotted line: $\sigma_y = \sigma_\infty + kd^{-1}$ with $\sigma_\infty = 100$ MPa and $k = 0.013$ MPa·$\mu$m; ⬡[4]; ⬠[5]; ◇[39]; ☆[6]; ⬠[40]; Δ[41]; ◇[42]; ◁[43]; ▽[44]; ▷[45]; ○[46]; × (Tabor relation)[5]; □ (Tabor relation).[47]

CG-Cu.[36] Despite this, it is seen that the both curves are in good agreement with the experimental data, indicating that the classical HP effect with the scaling exponent of 0.5 may not be the only model for describing the grain-size effect of submicron crystalline materials. In addition, the present curve can be equally represented by a similar relationship $\sigma_y = \sigma_\infty + kd^{-1}$ (dotted line in Figure 2). In fact, the power-law relation $\sigma_y = \sigma_\infty + kd^{-n}$ with $d$ the governing size and $n = 0.3 - 1$ is widely used for the size-dependent plasticity of metals when the governing size is in the submicron regime.[37] For instance, the micromechanical testing of micropillars shows that the yield stress of pillars scales to $d^{-1}$ rather than $d^{-0.5}$ where $d$ is the pillar diameter.[38] These observations lead to the suggestion that Eq. [2]

may be capable for describing the generalized size effect of crystalline materials.

The present model does not require extra assumptions such as the existence of dislocation pileups or high dislocation density, which nevertheless have been used to rationalize the HP law.[48] In addition, the present curve clearly shows a peak stress $\sigma_y \sim 900$ MPa at $d \sim 15$ nm, matching well with the highest ever reported values (see the data points in Figure 2). Further reducing the grain size leads to a stress plateau in our modeling result, consistent with the hardness ($H = 3\sigma_y$, Tabor relation) data of NG-Cu showing an unchanged yield strength with further decreasing $d$ below 15 nm. Such an observed phenomenon, however, will never be captured by the HP relationship (dashed line in Figure 2). Based on our modeling result, the stress plateau is attributed to a complete shift of the deformation mechanism, which will be discussed in the following paragraph. Note that the highest stress $\sigma_y \sim 900$ MPa is only about half the threshold stress $\hat{\sigma}_2 = M\hat{\tau}_2 = 1.8$ GPa (see Eq. [2]) for GB-mediated mechanism. This can be easily understood from the fact that $\hat{\sigma}_2$ is the mechanical threshold stress without the assistance of thermal activation, whereas $\sigma_y \sim 900$ MPa is obtained at room temperature. Indeed, molecular dynamics (MD) simulations[2] for NG-Cu at extremely high strain rates (thermal activation is suppressed) clearly demonstrate a flow stress as high as 2.25 GPa for $d = 15$ nm, in accord with $\hat{\sigma}_2 = 1.8$ GPa in our model.

To further understand the role of GBs on the overall strain rate for a given value of $d$, we denote $f_{GB} = \dot{\gamma}_{GB}/\dot{\gamma}$ as the portion of strain rate contributed by the GB-mediated deformation mechanism, where $\dot{\gamma}_{GB}$ and $\dot{\gamma}$ are defined in Eq. [2]. Similarly, $f_{disl} = 1 - f_{GB}$ is the strain rate contribution from conventional slip process. Figure 3 displays the variation of $f_{GB}$ *vs* $d$ based on the previous results (Figures. 1(b) and 2). When $d > 600$ nm, the overall strain rate $\dot{\gamma}$ is contributed exclusively by the dislocation activities, as clearly demonstrated by $f_{GB} \sim 0$ in this range. Due to the rapid decrease of $\phi$ starting at $d \sim 600$ nm (Figure 1(b)), $f_{GB}$ starts to increase but reaches only $\sim 0.18$ at $d \sim 400$ nm, followed by a plateau with relatively unchanged $f_{GB}$ in the UFG regime ($d > 100$ nm) despite further decreasing $d$. Meanwhile, the ratio $f_{disl}/f_{GB}$ is as high as $\sim 4.5$, suggesting that the conventional dislocation process still plays the dominant role in UFG metals. Interestingly, for UFG metals with $d < 400$ nm, the volume fraction $\phi$ is negligibly small (Figure 1(b)) compared to the large value of $f_{disl}$, suggesting that a small fraction of grains will deform much faster than the majority of grains in UFG metals. In other words, the dislocation activities and plastic strain will become inhomogeneous and locally favored in UFG metals, and this possibly corresponds to the formation of shear bands/zones during the straining of samples. This finding agrees well with experiments observing the shear localization in UFG/NG fcc metals.[5,32,44]

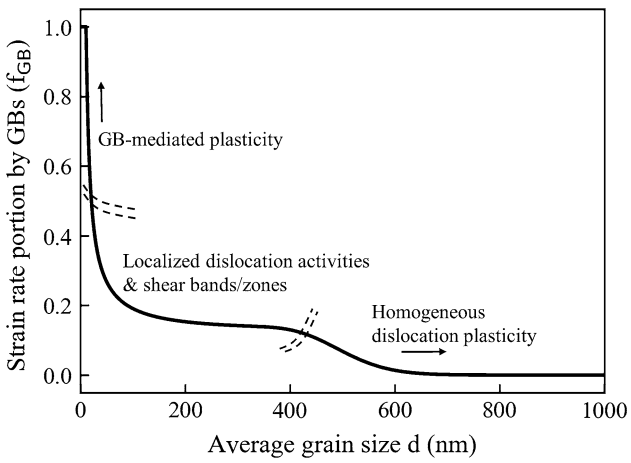


Fig. 3—Influence of average grain size on the fraction of strain rate provided by GB-mediated plasticity. The change of $f_{GB}$ with $d$ leads to three possible deformation behaviors roughly separated and shown in this figure.

When the grain size $d$ finally shifts from the UFG regime to the NG regime ($d < 100$ nm), $f_{GB}$ appears to "take off" and eventually reaches $f_{GB} = 1$ for $d \leq 15$ nm (Figure 3), indicating a complete transition of deformation mechanism from dislocation slip to the GB-mediated plasticity. This result is supported by MD simulations[13] showing that the majority of plastic deformation of NG-Cu with $d \sim 5$ nm is due to GB activities, with negligible part being caused by intragrain dislocation activities. Note that the dominance of GBs with $f_{GB} = 1$ also corresponds to the peak stress and the stress plateau in Figure 2. Therefore, our modeling result clearly demonstrates that such a dominant role played by GBs leads to the deviation from the traditional HP law, contrary to many proposals[5,49,50] attributing this deviation to the material defects such as porosities and impurities.[51]

Unlike the HP law incapable of predicting the SRS, the present work also captures the evolution of the overall value of $m$ with grain sizes. Since the $d$-dependent $\phi$ (Figure 1(b)) and $\sigma_y$ (Figure 2) are known, the values of $m$ at different grain sizes can be calculated using Eqs. [3] and [4]. The result of the predicted $m$ *vs* $d$, including the available data from the literature, is shown in Figure 4. The $m$ value has only increased slightly from 0.005 at CG scales to $\sim 0.01$ at UFG scale ($d = 100$ nm), despite $\phi \sim 0$ at this point. Again, this is due to the dominance of dislocations over GBs in terms of providing the strain rate (Figure 3), as discussed previously. With further decreasing $d$ into the NG regime, GBs become increasingly important and as a result, the value of $m$ starts to increase rapidly and reaches $\sim 0.25$ at $d \sim 25$ nm. Despite a little scattering of experimental data due possibly to the difficulty of accurately measuring $d$, the agreement between the experiments and the predicted trend of $m$ is certainly satisfactory.

Figure 4 highlights that even the GB-mediated plasticity characterized by $m_{GB} = 1$ becomes activated, the experimentally measured $m$ can still be significantly small. For example, $f_{GB} \sim 0.25$ for $d = 50$ nm (Figure 3), but the corresponding $m$ is as low as 0.02 (Figure 4), which is almost two orders of magnitude smaller than $m_{GB}$. In other words, the overall value of $m$

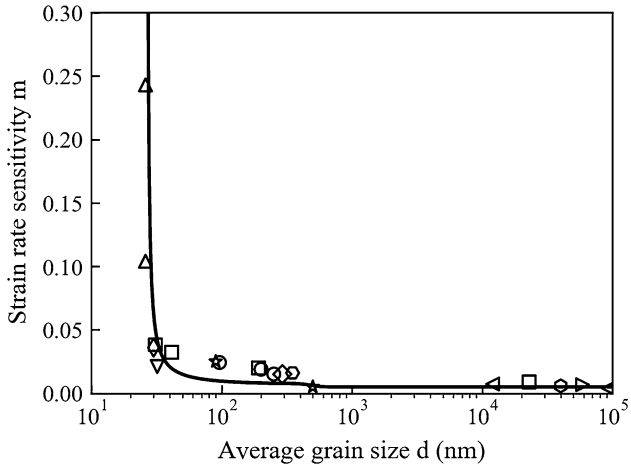


Fig. 4—The rate-sensitivity index *m vs d* (solid line) computed from Eq. [3], in comparison with experimental data (symbols) from literature for Cu with grain sizes ranging from CG regine to NG regine. ○[52]; □[23]; ◇[22]; △[53]; ◁[19]; ▷[54]; ⬠[55]; ☆[45]; ⬡[56]; ⬠[57]; △[26]; ▽.[39]

is hardly able to reflect $m_{GB}$ unless the grain size $d$ is truly controlled to be less than 15 nm (difficult to synthesize). This finding is not trivial, as it may provide the possible reason for the discrepancy between experiments (suggesting GBs are not important) and molecular dynamics simulations (observing the overwhelming role of GBs) on the deformation mechanisms of NG metals. Therefore, to experimentally probe the GB-related mechanism and properties in NG metals, one must ensure with carefulness that the grain sizes are truly in a few nanometers.

In summary, we have developed a crystal plasticity model incorporating both dislocation slip and GB-mediated mechanism to understand the rate-controlling deformation mechanisms of UFG/NG fcc metals. Grain size-related phenomenon such as the GB strengthening, the stress saturation and the evolution of strain rate sensitivity are all predicted well by this model. At small grain sizes, *i.e.*, several tens of nm, the statistical distributions of length scales (dislocation spacing and grain size) still allow room for localized dislocation activities occurred in some larger grains, which may lead to the low SRS and the shear bands observed in UFG/NG fcc metals. High SRS (*e.g.*, $>0.1$) seems unlikely even in NG metals unless the mean grain size is truly controlled below $\sim 15$ nm. Thus, the low SRS measured in NG metals may not indicate the absence of GB activities, and this result challenges many existing conclusions in literature.

## ACKNOWLEDGMENTS

M.X. Huang acknowledges the financial support from National Natural Science Foundation of China (Nos. U1764252, U1560204), National Key Research and Development Program of China (No. 2017YFB0304401) and Research Grants Council of Hong Kong (Nos. 17255016, 17203014, C7025-16G).

## REFERENCES

1. R. Armstrong: *Metal. Mater. Trans. B*, 1970, vol. 1B (5), pp. 1169–76.
2. J. Schiøtz and K.W. Jacobsen: *Science*, 2003, vol. 301 (5638), pp. 1357–59.
3. Z. Shan, E. Stach, J. Wiezorek, J. Knapp, D. Follstaedt, and S. Mao: *Science*, 2004, vol. 305 (5684), pp. 654–57.
4. L. Lu, Y. Shen, X. Chen, L. Qian, and K. Lu: *Science*, 2004, vol. 304 (5669), pp. 422–26.
5. P.G. Sanders, J. Eastman, and J. Weertman: *Acta Mater.*, 1997, vol. 45 (10), pp. 4019–25.
6. Y. Champion, C. Langlois, S. Guérin-Mailly, P. Langlois, J.-L. Bonnentien, and M.J. Hÿtch: *Science*, 2003, vol. 300 (5617), pp. 310–11.
7. E. Hall: *Proc. Phys. Soc. Sect. B*, 1951, vol. 64 (9), p. 747.
8. N. Petch: *J. Iron Steel Inst.*, 1953, vol. 174, pp. 25–28.
9. A. Lasalmonie and J. Strudel: *J. Mater. Sci.*, 1986, vol. 21 (6), pp. 1837–52.
10. G. Saada: *Mater. Sci. Eng. A*, 2005, vol. 400, pp. 146–49.
11. U. Kocks and H. Mecking: *Prog. Mater. Sci.*, 2003, vol. 48 (3), pp. 171–273.
12. K. Sieradzki, A. Rinaldi, C. Friesen, and P. Peralta: *Acta Mater.*, 2006, vol. 54 (17), pp. 4533–38.
13. J. Schiøtz, F.D. Di Tolla, and K.W. Jacobsen: *Nature*, 1998, vol. 391 (6667), p. 561.
14. H. Van Swygenhoven, M. Spaczer, A. Caro, and D. Farkas: *Phys. Rev. B*, 1999, vol. 60 (1), p. 22.
15. B. Zhu, R. Asaro, P. Krysl, K. Zhang, and J. Weertman: *Acta Mater.*, 2006, vol. 54 (12), pp. 3307–20.
16. Y. Ivanisenko, L. Kurmanaeva, J. Weissmueller, K. Yang, J. Markmann, H. Rösner, T. Scherer, and H.-J. Fecht: *Acta Mater.*, 2009, vol. 57 (11), pp. 3391–3401.
17. Y. Wang and E. Ma: *Appl. Phys. Lett.*, 2003, vol. 83 (15), pp. 3165–67.
18. I. Zhu, J. Li, A. Samanta, H.G. Kim, and S. Suresh: *Proc. Nat. Acad. Sci. USA*, 2007, vol. 104 (9), pp. 3031–36.
19. R. Carreker, Jr. and W. Hibbard, Jr: *Acta Metall.*, 1953, vol. 1 (6), pp. 654–63.
20. Y. Wang, A. Hamza, and E. Ma: *Acta Mater.*, 2006, vol. 54 (10), pp. 2715–26.
21. J. May, H. Höppel, and M. Göken: *Scripta Mater.*, 2005, vol. 53 (2), pp. 189–94.
22. L. Lu, S. Li, and K. Lu: *Scripta Mater.*, 2001, vol. 45 (10), pp. 1163–69.
23. J. Chen, L. Lu, and K. Lu: *Scripta Mater.*, 2006, vol. 54 (11), pp. 1913–18.
24. R.J. Asaro and S. Suresh: *Acta Mater.*, 2005, vol. 53 (12), pp. 3369–82.
25. R.J. Asaro and A. Needleman: *Acta Metall.*, 1985, vol. 33 (6), pp. 923–53.
26. Z. Jiang, X. Liu, G. Li, Q. Jiang, and J. Lian: *Appl. Phys. Lett.*, 2006, vol. 88 (14), p. 143115.
27. B. Zhu, R. Asaro, P. Krysl, and R. Bailey: *Acta Mater.*, 2005, vol. 53 (18), pp. 4825–38.
28. E. Gürses and I. El Sayed: *J. Mech. Phys. Sol.*, 2011, vol. 59 (3), pp. 732–49.
29. G. Lemoine, L. Delannay, H. Idrissi, M.-S. Colla, and T. Pardoen: *Acta Mater.*, 2016, vol. 111, pp. 10–21.
30. F. Dalla Torre, H. Van Swygenhoven, and M. Victoria: *Acta Mater.*, 2002, vol. 50 (15), pp. 3957–70.
31. H. Van Swygenhoven: *Science*, 2002, vol. 296 (5565), pp. 66–67.
32. S. Cheng, E. Ma, Y. Wang, L. Kecskes, K. Youssef, C. Koch, U. Trociewitz, and K. Han: *Acta Mater.*, 2005, vol. 53 (5), pp. 1521–33.
33. Y. Wei, A.F. Bower, and H. Gao: *Acta Mater.*, 2008, vol. 56 (8), pp. 1741–52.
34. S. Nemat-Nasser and Y. Li: *Acta Mater.*, 1998, vol. 46 (2), pp. 565–77.
35. M. Soare and W. Curtin: *Acta Mater.*, 2008, vol. 56 (15), pp. 4046–61.
36. K.K. Chawla and M. Meyers: *Mechanical Behavior of Materials*, Prentice Hall, Upper Saddle River, 1999.
37. T. Zhu, A. Bushby, and D. Dunstan: *Mater. Technol.*, 2008, vol. 23 (4), pp. 193–209.
38. D. Dunstan and A. Bushby: *Int. J. Plast.*, 2013, vol. 40, pp. 152–62.

39. A.S. Khan, B. Farrokh, and L. Takacs: *J. Mater. Sci.*, 2008, vol. 43 (9), pp. 3305–13.
40. M. Legros, B. Elliott, M. Rittner, J. Weertman, and K. Hemker: *Philos. Mag. A*, 2000, vol. 80 (4), pp. 1017–26.
41. R.S. Iyer, C.A. Frey, S. Sastry, B. Waller, and W. Buhro: *Mater. Sci. Eng. A*, 1999, vol. 264 (1–2), pp. 210–14.
42. V. Gertsman, M. Hoffmann, H. Gleiter, and R. Birringer: *Acta Metall. Mater.*, 1994, vol. 42 (10), pp. 3539–44.
43. K.M. Youssef, R.O. Scattergood, K. Linga Murty, and C.C. Koch: *Appl. Phys. Lett.*, 2004, vol. 85 (6), pp. 929–31.
44. Y. Wang, K. Wang, D. Pan, K. Lu, K. Hemker, and E. Ma: *Scripta Mater.*, 2003, vol. 48 (12), pp. 1581–86.
45. L. Lu, R. Schwaiger, Z. Shan, M. Dao, K. Lu, and S. Suresh: *Acta Mater.*, 2005, vol. 53 (7), pp. 2169–79.
46. D. Das, A. Samanta, and P. Chattopadhyay: *Mater. Manuf. Process.*, 2006, vol. 21 (7), pp. 698–702.
47. G. Fougere, J. Weertman, R. Siegel, and S. Kim: *Scripta Metall. Mater.*, 1992, vol. 26 (12), pp. 1879–83.
48. Z. Cordero, B. Knight, and C. Schuh: *Int. Mater. Rev.*, 2016, vol. 61 (8), pp. 495–512.
49. M. Dollár and A. Dollár: *J. Mater. Process. Technol.*, 2004, vol. 157, pp. 491–95.
50. F. Yin, GJ. Cheng, R. Xu, K. Zhao, Q. Li, J. Jian, S. Hu, S. Sun, L. An, and Q. Han: *Scripta Mater.*, 2018, vol. 155, pp. 26–31.
51. E. Ma: *Scripta Mater.*, 2003, vol. 49 (7), pp. 663–68.
52. Q. Wei, S. Cheng, K. Ramesh, and E. Ma: *Mater. Sci. Eng. A*, 2004, vol. 381 (1–2), pp. 71–79.
53. G. Gray, III, T. Lowe, C. Cady, R. Valiev, and I. Aleksandrov: *Nanostruct. Mater.*, 1997, vol. 9 (1–8), pp. 477–80.
54. M. Zehetbauer and V. Seumer: *Acta Metall. Mater.*, 1993, vol. 41 (2), pp. 577–88.
55. W. Bochniak: *Acta Metall. Mater.*, 1995, vol. 43 (1), pp. 225–33.
56. P. Follansbee and U. Kocks: *Acta Metall.*, 1988, vol. 36 (1), pp. 81–93.
57. Y. Li, X. Zeng, and W. Blum: *Acta Mater.*, 2004, vol. 52 (17), pp. 5009–18.